First Observation of the Point Spread Function of Optical Transition Radiation

Pavel Karataev,[1,*] Alexander Aryshev,[2] Stewart Boogert,[1] David Howell,[3] Nobuhiro Terunuma,[2] and Junji Urakawa[2]

[1]John Adams Institute at Royal Holloway, University of London, Egham, Surrey, TW20 0EX, United Kingdom
[2]KEK: High Energy Accelerator Research Organization, 1-1 Oho, Tsukuba, Ibaraki 305-0801, Japan
[3]John Adams Institute at University of Oxford, Keble Road, Oxford, OX1 3RH, United Kingdom

(Received 30 October 2009; published 17 October 2011)

We represent the first experimental observation of the point spread function (PSF) of optical transition radiation (OTR) performed at KEK-Accelerator Test Facility extraction line. We have demonstrated that the PSF vertical polarization component has a central minimum with a two lobe distribution. However, the distribution width varied significantly with wavelength. We assume that we observed a severe effect from spherical or chromatic aberrations which are not taken into account in any existing theoretical model. We believe that the result of this work will encourage theoreticians to continue developing the theory as it is important for various transition radiation applications. Nonuniform distribution of the OTR PSF creates an opportunity for developing a submicrometer transverse beam size monitor.

DOI: 10.1103/PhysRevLett.107.174801 PACS numbers: 41.60.−m, 41.75.Ht

Transition radiation (TR) appearing when a charged particle crosses a boundary between two media with different dielectric constants (or vacuum-metal interface) has widely been used for various applications such as transverse charged particle beam profile, emittance and position diagnostics [1,2], energy spread and bunch length measurements [3,4], generation of intense THz and sub-THz radiation beams [5], and in transition radiation trackers for particle detection [6]. For many applications the TR source generated by a single electron has been considered as a point. However, when TR is used for THz radiation generation, the wavelength is very long and the single electron source size (with effective value of order of $\gamma\lambda$, where λ is the radiation wavelength and γ is the charged particle Lorentz-factor) can reach macroscopic dimensions which can even exceed the target size. If the single electron size distribution is comparable to or larger than the TR target, then even when observing the radiation at infinity the TR spectral-angular characteristics significantly depend on the target dimensions; i.e., the TR source generated by a single electron cannot be treated as a point [7].

TR in optical wavelength range (OTR) is used for transverse electron beam profile diagnostics. The resolution of the OTR monitors is normally defined as a root-mean-square of the so-called OTR point spread function (PSF) [8]. By definition the OTR PSF is a source distribution generated by a single electron and projected by an optical system on a detector. Therefore, the PSF contains information about both actual source distribution at the target surface and imperfections of the optical system.

There are a couple theoretical treatments of an OTR source distribution. In [8] the authors used a McDonald function based distribution for OTR source description which was derived in [9]. The function has a divergence to infinity at zero distance from the particle trajectory (see Fig. 1). In [10] the authors used the theory based on Huygens principle of wave diffraction. They assumed that the photons closer to the particle trajectory than the radiation wavelength could not be converted into real ones and, therefore, obtained the following approximated formula for an azimuthally symmetric OTR source distribution:

$$I_{\mathrm{PSF}}(x, y) = \mathrm{const} \times \left| \alpha K_1(\alpha\rho) - \frac{J_0(k\rho)}{\rho} \right|^2. \quad (1)$$

Here $\rho = \sqrt{x^2 + y^2}$ and x and y are orthogonal coordinates of the target surface; $k = 2\pi/\lambda$ is the wave number; $\alpha = k/\gamma$; J_0 is the Bessel Function and K_1 is the McDonald or modified Bessel Function.

In contrast to the model used in [8,9] Eq. (1) has an additional term containing a Bessel function. It results in the appearance of a central minimum distribution (see Fig. 1) and a peak half a wavelength away from the particle trajectory.

The distribution on a detector will be defined by OTR PSF which depends on the OTR source distorted during the measurements by such phenomena as diffraction of the TR tails propagating through a narrow aperture, chromatic and spherical aberrations of a focusing lens, or even sensitivity

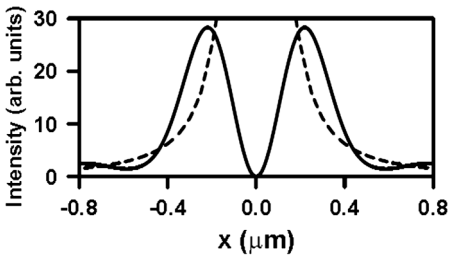

FIG. 1. OTR source calculated using two approaches presented in [8,9] (dashed line) and [10] Eq. (1) (solid line). ($\gamma = 2500$, $\lambda = 500$ nm, $x = 0$, and const = 1.)

TABLE I. ATF II beam parameters [12].

Energy	1.28 GeV ($\gamma = 2500$)
Vertical emittance	2.5×10^{-11} m rad
Horizontal emittance	2.0×10^{-9} m rad
Bunch population	1.0×10^{10}
Bunch length	~8 mm

of a measurement system. Unfortunately, the existing theoretical approaches allow us to take into account the diffraction effect only. Both approaches presented in Fig. 1 were used for estimations of the PSF distortion due to diffraction in [8,10]. However, they produce a different result only when the angular aperture of the measurement system is comparable to unity. Both methods predict that the PSF has radial polarization, a central minimum, and its width is reduced when the radiation wavelength decreases [8].

Although the PSF might be considerably larger than the actual source distribution, its dimensions might still be very small. One of the challenges to measure the OTR PSF experimentally and observe its structure is that it is very difficult to squeeze an electron beam down to the dimensions much smaller than the PSF. We performed an experiment on the observation and investigation of the OTR PSF at KEK-Accelerator Test Facility ATF II beam line [11]. KEK-ATF is an 1.28 GeV damping ring which produces an extremely low emittance beam (see Table I). It allows us to squeeze the electron beam down to submicrometer dimensions at almost any location in the extraction line.

The OTR system was integrated into the laser wire system being constructed at ATF II [11,13]. The $30 \times 30 \times 0.3$ mm aluminized silicon target was mounted on a 4D vacuum manipulator. Vertical translation and rotation around the vertical axis were automated and remotely controlled. The target was placed at 45° to the beam trajectory and the generated OTR was extracted through a fused silica viewport.

The optical system consisted of a focusing lens with focus $f = 100$ mm, a polarizer, and an optical filter placed in front of the detector. The diameter of the lens was chosen to be 50.8 mm to minimize the diffraction effect predicted by the theory. A set of optical filters (459 ± 18 nm, 558 ± 20 nm, and 609 ± 18 nm) was used in the experiment. Two aluminum mirrors formed a periscope and reflected the OTR light under the vacuum chamber in order to minimize the beam based background and to achieve a large magnification factor (see Fig. 2). Two orientation axes of one of the mirrors were automated and remotely controlled for beam based tuning of the optical system. An initial alignment was performed using a former ODR alignment system well described in [14]. A vacuum mirror installed upstream reflected a 632.8 nm laser light generated by a helium-neon laser along the electron beam path (see Fig. 2). Reflecting the laser light

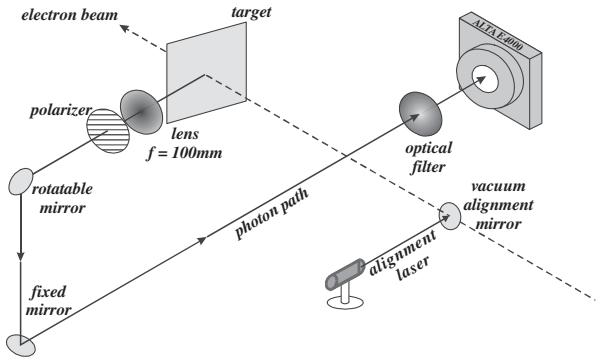

FIG. 2. Experimental layout.

from the OTR target we were able to align the optical system. As a detector we used a 16 bit highly sensitive (QE ~50%) cooled CCD camera (ALTA E4000, with 7.4 μm square pixels).

The vertical position of the target was precisely monitored by the manipulator position readout system. Measuring the position shift of the target edge at the CCD camera as a function of the manipulator readout we could calibrate the optical system and determine its magnification factor. The calibration curve is represented in Fig. 3. As is seen a large magnification factor $M = 18.87$ was achieved.

The electron beam optics optimized using the SAD code [15] predicted the beam size in the waist to be $\sigma_y = 1.73$ μm—vertical and $\sigma_x = 23.04$ μm—horizontal. Vertical and horizontal beam sizes could also be changed by two nearest quadrupole magnets and predicted by SAD. According to the theory the vertical polarization component is significantly affected by the vertical beam size, and the horizontal one—by the horizontal beam size. Since the horizontal beam size is much larger than the vertical one it could smooth the OTR image completely eliminating the central minimum. In order to prevent this the polarizer was orientated for measurement of vertical polarization component.

A few examples of experimental OTR PSF images of vertical polarization component measured in the electron beam waist with different optical filters are represented in Fig. 4. The number of generated OTR photons and the

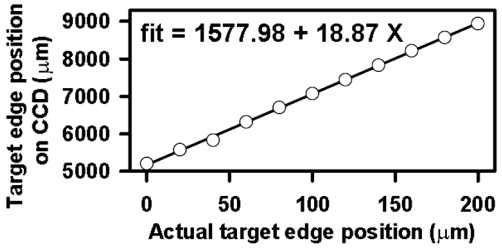

FIG. 3. Calibration curve: A linear fit is shown on the picture. The magnification factor is $M = 18.87 \pm 0.18$ derived from the fit.

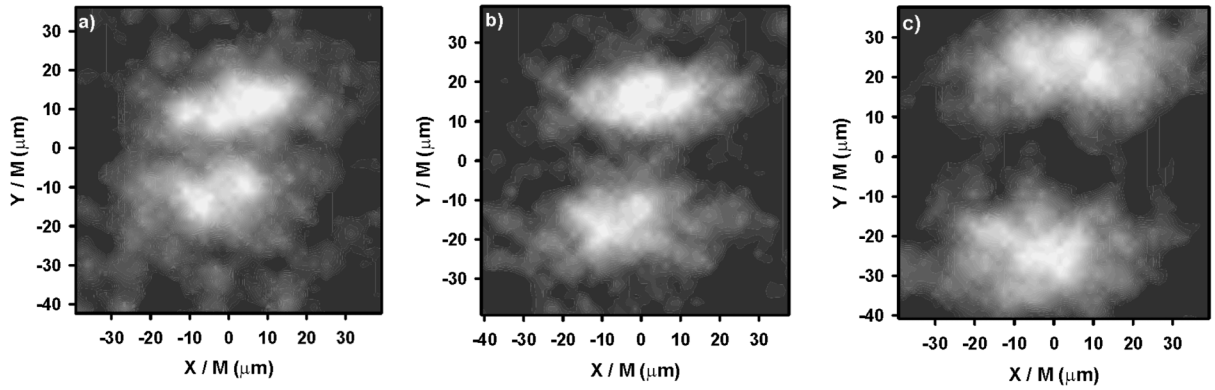

FIG. 4 (color online). CCD Images taken with three different optical filters: (a) −609 nm; (b) −558 nm; (c) −459 nm.

photon density at the CCD was enough to perform single-shot measurements. One may see that the OTR PSF has a two lobe distribution with a clear central minimum, which was predicted by the theory. However, the existing theory takes into account the diffraction of the TR tails only; i.e., the diffraction effect is smaller for shorter wavelength. According to [8] for the angular aperture of 0.254 rad defined by the lens diameter of 50.8 mm and focusing distance of 0.1 m the distribution represented in Fig. 1 must be broadened by a factor of 3 due to diffraction effect. In Fig. 5 one may see that the distribution width increases when reducing the radiation wavelength, which contradicts the theoretical expectation. Moreover, the peak-to-peak distance is 100 times larger than it was predicted by the theory. We assume the discrepancy appears due to severe chromatic and spherical aberrations in the optical lens. Large lens aperture has lead to a very small diffraction effect, but it has introduced chromatic and spherical aberrations. Since the alignment of the optical system was done using a red laser (632 nm), the minimal distribution width corresponds to the 609 nm wavelength (red) filter. Figure 5 (left) represents projections of the distributions presented in Figs. 4(a) and 4(c). The root-mean-square (rms) of the distribution has always been considered as a resolution for conventional OTR beam profile monitors. The measured rms and peak-to-peak distance of the OTR distribution as a function of wavelength is represented in Fig. 5 (right). One may see that the distribution width increases when the wavelength decreases. This results clearly demonstrate that to be able to precisely estimate the resolution of an optical system for modern accelerators, where a few micrometer resolution is required, the chromatic and spherical aberrations must be taken into account. The effect of the chromatic and spherical aberration has been estimated using a sophisticated ZEMAX code used for optics calculations [16]. The results were quantitatively consistent with the measurements.

One should say that the PSF visibility significantly depends on the vertical size of the beam. A very small beam size was required to observe the clear OTR PSF structure. Figure 6 represents the OTR PSF measured for two beam sizes. One may see when the beam size changes from 1.7 to 4 μm as predicted by SAD code the PSF visibility reduced by a factor of 2. The further increase of the beam size results in complete smoothing of the PSF structure. When the beam size was much larger than the OTR PSF we directly measured the beam profile; i.e., the system became a conventional OTR beam profile monitor.

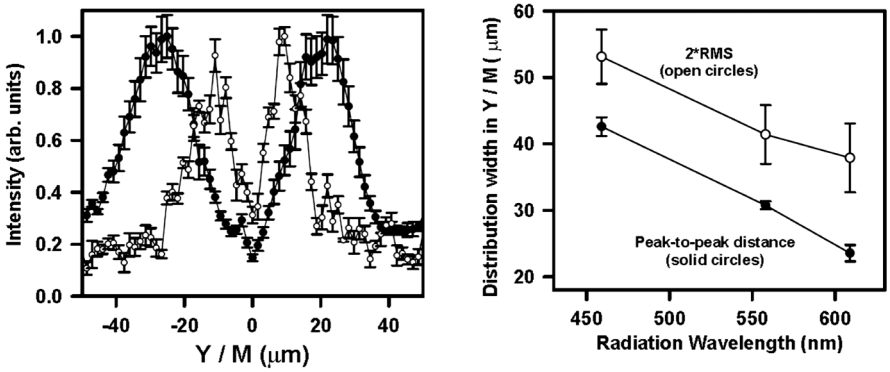

FIG. 5. OTR projections (left) demonstrated in Fig. 4(a) (open circles) and Fig. 4(c) (solid circles) and the distribution widths (right): solid circles—peak-to-peak distance and open circles—doubled rms width calculated using the second momentum method. The error bars are statistical obtained from averaging over 5 shots.

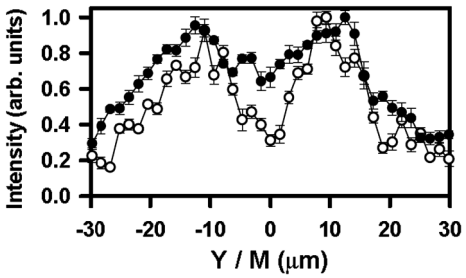

FIG. 6. Two OTR distributions measured with 609 nm optical filter for two current settings of QD18X quadruple magnet. Open circles—$I_{QD18X} = 29.61$ A and solid circles—$I_{QD18X} = 29.91$ A corresponding to SAD calculation of the vertical beam size to be $\sigma_y = 1.73$ μm and $\sigma_y = 4.03$ μm respectively.

The change in the visibility might be used to extract the information about the beam size with micrometer or even submicrometer resolution if the effect of spherical and chromatic aberrations is minimized. Up-to-date it was believed that the resolution of the OTR beam profile monitors is defined by the diffraction limit. The results presented in this Letter clearly demonstrate that even if the OTR PSF width is diffraction limited, its distribution is nonuniform. The behavior of the PSF structure gives an opportunity to measure smaller beam sizes.

In this Letter we have represented the first observation and investigation of the point spread function in optical transition radiation at an extremely low emittance electron beam at KEK-ATF2 beam line. We have clearly observed a two lobe distribution with a clear minimum in the center. A severe effect from chromatic and spherical aberrations was observed, which significantly affects the resolution for the OTR beam size monitors. We believe the results of this experiment give a foundation for better understanding of the transition radiation origin and will encourage theoreticians to develop a more advanced theoretical model which will help to estimate the resolution for beam size monitors which is the most famous OTR application in modern accelerators.

The obvious application of the PSF structure is for beam diagnostics. Initially submicrometer resolution from OTR PSF might allow us to cross-check both the laser interferometer [17] and the micron-scale laser wire system [13] being developed at KEK-ATF2 beam line [11]. Furthermore, it can also be used and an independent diagnostics in its own right for submicron beam size measurements. The diagnostics aspects of the research will be considered in a successive paper.

We would like to express our gratitude to all members of the Laser Wire Collaboration and ATF/ATF2 Group for their helpful support. This research was partially supported by DAIWA Anglo-Japanese Foundation.

*Corresponding author.
karataev@pp.rhul.ac.uk

[1] R. B. Fiorito and D. W. Rule, in *Proceedings of the Beam Instrumentation Workshop, Santa Fe, 1993*, edited by R. E. Shafer, AIP Conf. Proc. No. 319 (AIP, New York, 1994), p. 21.
[2] M. Manclossi, J. J. Santos, D. Batani, J. Faure, A. Debayle, V. T. Tikhonchuk, and V. Malka, Phys. Rev. Lett. **96**, 125002 (2006).
[3] Y. Glinec, J. Faure, A. Norlin, A. Pukhov, and V. Malka, Phys. Rev. Lett. **98**, 194801 (2007).
[4] G. A. Krafft, J.-C. Denard, R. W. Dickson, and R. Kazimi, arXiv:physics/0009087.
[5] Y. Shibata, K. Ishi, S. Ono, Y. Inoue, S. Sasaki, M. Ikezawa, T. Takahashi, T. Matsuyama, K. Kobayashi, Y. Fujita, and E. G. Bessonov, Phys. Rev. Lett. **78**, 2740 (1997).
[6] G. Hartmann, D. Muller, and T. Prince, Phys. Rev. Lett. **38**, 1368 (1977).
[7] P. Karataev, S. Araki, R. Hamatsu, H. Hayano, T. Muto, G. Naumenko, A. Potylitsyn, N. Terunuma, and J. Urakawa, Nucl. Instrum. Methods Phys. Res., Sect. B **227**, 198 (2005).
[8] M. Castellano and V. A. Verzilov, Phys. Rev. ST Accel. Beams **1**, 062801 (1998).
[9] M. L. Ter-Mikaelyan, *High Energy Electromagnetic Processes in Condensed Media* (Wiley Interscience, New York, 1972).
[10] M. Castellano, A. Cianchi, G. Orlandi, and V. A. Verzilov, Nucl. Instrum. Methods Phys. Res., Sect. A **435**, 297 (1999).
[11] A. Seryi *et al.*, in *Proceedings of the 2009 Particle Accelerator Conference, Vancouver, Canada* (IEEE, Piscataway, NJ, 2009).
[12] K. Kubo *et al.*, Phys. Rev. Lett. **88**, 194801 (2002).
[13] A. Aryshev *et al.*, in *Proceedings of the 2009 Particle Accelerator Conference, Vancouver, Canada* (Ref. [11]).
[14] P. Karataev, S. Araki, A. Aryshev, G. Naumenko, A. Potylitsyn, N. Terunuma, and J. Urakawa, Phys. Rev. ST Accel. Beams **11**, 032804 (2008).
[15] SAD, Strategic Accelerator Design, http://acc-physics.kek.jp/SAD/sad.html.
[16] "ZEMAX: software for optical design," http://www.zemax.com.
[17] V. Balakin *et al.*, Phys. Rev. Lett. **74**, 2479 (1995).